

Potentiometric Measurement of Intracellular Redox Activity

Joshua D. Rabinowitz, Judith F. Vacchino, Craig Beeson,[†] and Harden M. McConnell*

Contribution from the Department of Chemistry, Stanford University, Stanford, California 94035

Received October 13, 1997. Revised Manuscript Received December 8, 1997

Abstract: Living cells typically contain numerous redox couples such as NAD⁺/NADH, NADP⁺/NADPH, cystine/cysteine, and the oxidized and reduced forms of glutathione and metalloenzymes. It is expected that the intracellular concentrations of these couples may change selectively with changes in the cellular environment, such as those due to hormones, growth factors, and nutrients. The present work employs an electrochemical potentiometric means of probing intracellular redox activity in live cells. The couple menadione/menadiol is used as a carrier mediator, carrying electrons across the cell membrane, and sensing intracellular redox enzyme activity. The extracellular menadiol redox activity is monitored by means of an extracellular solution containing the ferricyanide/ferrocyanide couple and a gold electrode. Evidence is presented that the extracellular rate of reduction of ferricyanide is limited by the intracellular rate of reduction of menadione. A substantial fraction (30–80% depending on cell type) of ferricyanide reduction is mediated by DT-diaphorase-catalyzed transfer of electrons from NADPH to menadione. Reduction of menadione and oxidation of menadiol by enzymes of the mitochondrial electron transport chain also contribute to the observed ferricyanide reduction rate. Some membrane receptor agonists increase the ferricyanide reduction rate, whereas others decrease this rate, demonstrating specific hormonal regulation of cellular redox enzyme activity.

Introduction

Metabolic pathways in living cells are tightly regulated and highly sensitive to cellular needs. All of the major metabolic pathways in cells involve redox reactions and specific redox couples that cycle between oxidized and reduced states. The concentrations of the redox couples help regulate the flow of metabolites through these pathways.^{1,2} Moreover, recent evidence suggests that the concentrations of specific redox couples may play a role in the regulation of other cellular functions. These include the transcription of DNA into mRNA,³ the translation of mRNA into proteins,⁴ and the activity of signal transduction enzymes.^{5,6}

An interesting aspect of the tight control of cellular metabolism is that cellular metabolic rates are often responsive to receptor agonists even when there is no evident connection between receptor function and metabolism. As one example, the binding of carbachol to the muscarinic acetyl choline receptor leads to an enhanced rate of extracellular acid excretion.⁷ Numerous additional examples can be found in the literature where acid release is taken as a measure of metabolic rate enhancement.⁸ In many cases this additional acid release

may be due to enhanced glycolytic metabolism in response to an increased ATP demand.

The same line of reasoning has suggested to us that the intracellular concentrations of redox couples may likewise be responsive to receptor agonists, as well as cell nutrients. In principle, assays for such concentration changes can be made by using chemical analysis of cell lysates. For example, biochemical techniques exist for the direct quantitation of NAD⁺/NADH, NADP⁺/NADPH, cystine/cysteine, and oxidized/reduced glutathione (γ -glutamylcysteinylglycine, GSSG/GSH). However, spectroscopic or potentiometric methods offer the possibility of convenient, serial measurements of redox enzyme activity in live cells. One complication for all such measurements is that there are numerous intracellular redox couples, each of which may reside at different redox potentials. For example, in eukaryotic cells the ratio (NAD⁺/NADH) is generally some 10⁵ times larger than the ratio (NADP⁺/NADPH) even though these couples have nearly the same redox potentials.^{9–12} Moreover, for any one redox pair, different potentials may be maintained in different subcellular compartments.¹³

In the present work we have used an extracellular potentiometric measurement to probe the intracellular redox reactivity of living cells. The redox couple menadione/menadiol (2-methyl-1,4-naphthalenedione/2-methyl-1,4-naphthalenediol) serves as a carrier mediator. This redox couple is an effective carrier of electrons across lipid membranes because both menadione

* To whom correspondence should be addressed.

[†] Current address: Department of Chemistry, University of Washington, Seattle, WA 98195.

(1) Stryer, L. *Biochemistry*; W. H. Freeman and Company: New York, 1995; pp 443–652.

(2) Buchanan, B. B. *Arch. Biochem. Biophys.* **1991**, *288*, 1–9.

(3) Abate, C.; Patel, L.; Rauscher, F. J.; Curran, T. *Science* **1990**, *249*, 1157–1161.

(4) Danon, A.; Mayfield, S. P. *Science* **1994**, *266*, 1717–1719.

(5) Wang, X.; Culotta, V. C.; Klee, C. B. *Nature* **1996**, *383*, 434–437.

(6) Yu, L.; Haddy, A.; Rusnak, F. *J. Am. Chem. Soc.* **1995**, *117*, 10147–10148.

(7) Owicki, J. C.; Parce, J. W.; Kercso, K. M.; Sigal, G. B.; Muir, V. C.; Venter, J. C.; Fraser, C. M.; McConnell, H. M. *Proc. Natl. Acad. Sci. U.S.A.* **1990**, *87*, 4007–4011.

(8) McConnell, H. M.; Owicki, J. C.; Parce, J. W.; Miller, D. L.; Baxter, G. T.; Wada, H. G.; Pitchford, S. *Science* **1992**, *257*, 1906–1912.

(9) Williamson, J. R.; Corkey, B. E. *Methods Enzymol.* **1969**, *13*, 434–510.

(10) Williamson, J. R.; Corkey, B. E. *Methods Enzymol.* **1979**, *55*, 200–222.

(11) Tischler, M. E.; Friedrichs, D.; Coll, K.; Williamson, J. R. *Arch. Biochem. Biophys.* **1977**, *184*, 222–236.

(12) Veech, R. L.; Eggleston, L. V.; Krebs, H. A. *Biochem. J.* **1969**, *115*, 609–619.

(13) Hwang, C.; Sinskey, A. J.; Lodish, H. F. *Science* **1992**, *257*, 1496–1502.

and menadiol are lipid soluble.¹⁴ Menadione and menadiol are mediators in that they are oxidized and/or reduced by intracellular enzymes. The external medium bathing the cells is chosen to contain the ferricyanide/ferrocyanide couple. Ferricyanide reacts rapidly with menadiol. The extracellular potential of the ferricyanide/ferrocyanide couple is measured with a gold electrode. The rate of extracellular ferricyanide reduction is thus a measure of intracellular redox activity. Our results indicate that under basal conditions a substantial proportion of the intracellular reduction of menadione is due to NADPH and mediated by DT-diaphorase (EC 1.6.99.2), an enzyme that catalyzes the transfer of electrons from either NADH or NADPH to quinones such as menadione. In addition, the net amount of menadione reduction is sensitive to mitochondrial electron transport chain reactions.

Experimental Approach

To implement the potentiometric method mentioned above, we have used a modified Cytosensor microphysiometer. The essential features of the microphysiometer system are that it allows a moderate number of cells ($\approx 10^5$) to be trapped in a small volume ($\approx 10 \mu\text{L}$) that is in contact with electrodes. In addition, flow through the sensing chamber containing the cells can be controlled, and the sensing chamber can be rinsed completely in only a few seconds. The microphysiometer was originally designed to detect signal transduction cascades based on changes in the rate at which cells secrete acidic metabolites.⁸ In it, the pH of fluid bathing cells is measured with a potentiometric silicon-based electrode. In the modified instrument, the pH-sensing electrode is replaced by a gold electrode¹⁵ (Figure 1). This electrode consists of a layer of gold separated from a silicon semiconductor by an insulating layer of silicon oxynitride. The electrochemical potential at the gold–electrolyte interface contributes to the reverse-bias potential acting across the photosensitive silicon semiconductor. Illumination of the silicon with a light-emitting diode creates hole–electron pairs which are separated in the potential gradient in the silicon. This generates an ac photocurrent in the external circuit. The dependence of this current on the voltage applied by the controlling electrode is used to determine changes in the redox potential at the gold surface. No measurable (≥ 1 pA) direct current flows through the circuit during these measurements. This electrode design allows stable, rapid, low-noise measurements on microliter volumes.¹⁵

Measurement of the redox activity of the interior of cells requires a carrier mediator to link the extracellular electrolyte solution to intracellular redox pairs. The essential requirement of this couple is that it will exchange electrons rapidly with both the exterior and the interior couple. We find that this requirement is met by the menadione/menadiol couple (Figure 2A).¹⁶ The menadione/menadiol couple can transfer electrons across a lipid bilayer to a ferricyanide/ferrocyanide redox buffer in a cell-free system.¹⁴ In one plausible reaction cycle, menadione (M) undergoes a two-electron reduction to form menadiol, with a cellular component such as NAD(P)H as the reducing source^{17–19} (Figure 2A). Menadiol then leaves the

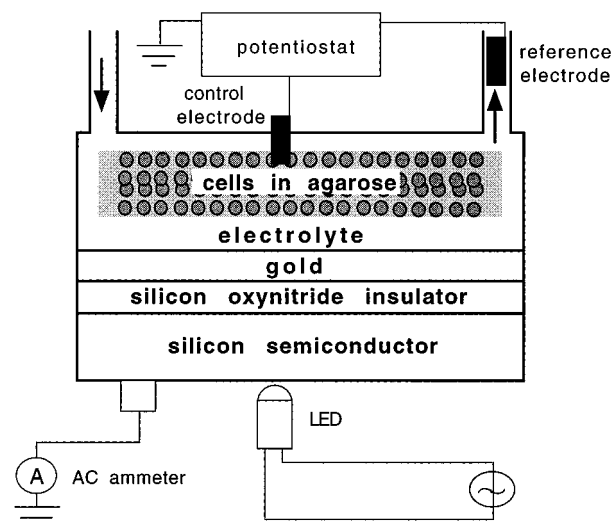


Figure 1. Light-addressable potentiometric gold electrode. The electrode consists of a layer of gold separated from a silicon semiconductor by an insulating layer of silicon oxynitride. The gold is in contact with an electrolyte solution loaded with cells contained in an agarose matrix (gray area) on top of a microporous polycarbonate membrane (not shown). Flow through the sensing chamber is controlled by a peristaltic pump. Arrows depict the flow inlet and outlet. A control electrode modulates the potential across the reverse-biased semiconductor. An ac-photocurrent is generated when a light-emitting diode (LED) illuminates the silicon. The dependence of this current on the voltage applied by the controlling electrode is used to determine changes in the redox potential at the gold surface. The figure is not to scale.

cell and reduces ferricyanide in the external media to ferrocyanide, regenerating menadione (see Figure 2B).¹⁴ Another possible reaction cycle involves one-electron reduction of menadione to a semiquinone radical, which might also leave the cell and reduce ferricyanide.^{17–19} Other reactions of menadione which may occur in cells are discussed in the Experimental Section.^{20,21}

Figure 2C shows that the external gold electrode in the ferricyanide/ferrocyanide solution tracks at least one intracellular redox reaction. Prior to the addition of menadione, the potential of the external solution is nearly constant. In the absence of cells, addition of menadione has no effect on the potential. In the presence of cells, addition of menadione causes a change in the measured potential consistent with ferricyanide reduction. We term such a change as “positive”. In the presence of both cells and menadione, the potential oscillates when the sensing chamber is periodically perfused with fresh medium (by turning on and off a peristaltic pump). The most rapid positive change in potential occurs during last 10 s of the no-perfusion (pump off) period. We term the rate of change in potential during this time (i.e., the steepest positive slope of the oscillations in Figure 2C) as the “reduction rate”. Through the Nernst equation, this rate ($\mu\text{V s}^{-1}$) can be converted into a molar rate of ferricyanide reduction ($\mu\text{M s}^{-1}$) when the initial concentrations of both ferricyanide and ferrocyanide are known.

Menadione Cycle. Menadione mediates the transfer of electrons from the inside of cells to ferricyanide (Figure 2C).

(14) Grimaldi, J. J.; Boileau, S.; Lehn, J. M. *Nature* **1977**, *265*, 229–230.

(15) Hafeman, D. G.; Parce, J. W.; McConnell, H. M. *Science* **1988**, *240*, 1182–1185.

(16) In preliminary experiments, C.B. has found furazone compounds are also effective carrier mediators and can be used to probe different redox reactions from menadione.

(17) Thor, J.; Smith, M. T.; Hartzell, P.; Bellomo, G.; Jewell, S. A.; Orrenius, S. *J. Biol. Chem.* **1982**, *257*, 12419–12425.

(18) Lind, C.; Hochstein, P.; Ernster, L. *Arch. Biochem. Biophys.* **1982**, *216*, 178–185.

(19) Iyanagi, T.; Yamazaki, I. *Biochim. Biophys. Acta* **1970**, *216*, 282–294.

(20) Fieser, L. F.; Turner, R. B. *J. Am. Chem. Soc.* **1947**, *69*, 2335–2338.

(21) Nickerson, W. J.; Falcone, G.; Strauss, G. *Biochemistry* **1963**, *2*, 537–546.

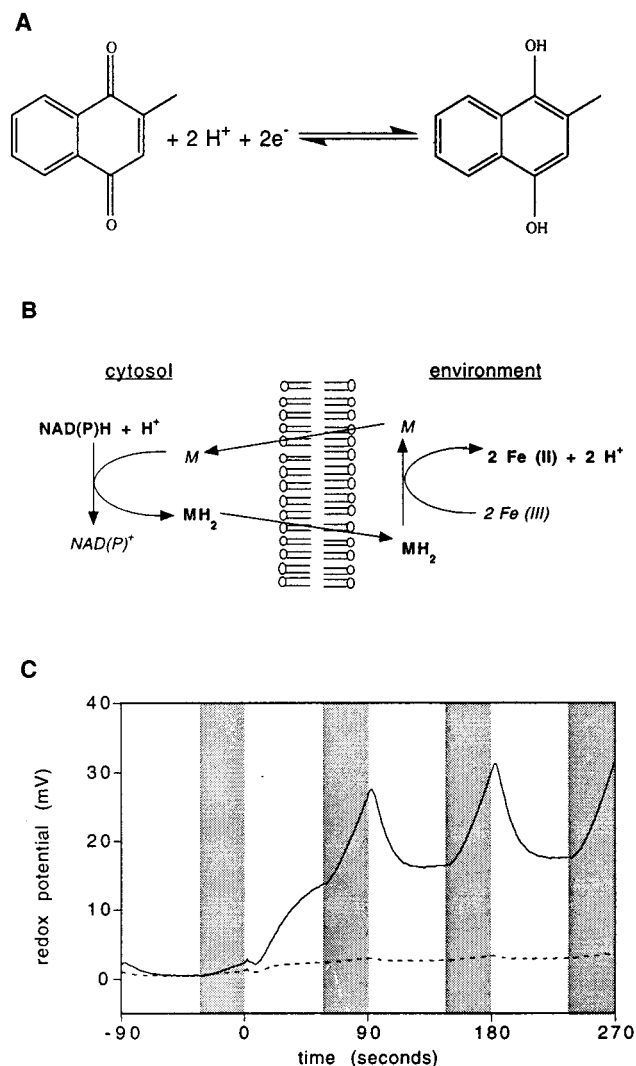


Figure 2. Detection of cellular redox reactions with use of menadione to link intra- and extracellular redox pairs. (A) Two-electron reduction of menadione to menadiol. (B) Hypothetical menadione reaction cycle. Menadione (M) diffuses into a cell, where it is reduced to menadiol (MH₂). Menadiol (MH₂) then diffuses out of the cell and reacts with ferricyanide, labeled for simplicity Fe(III), converting it into ferrocyanide, labeled Fe(II), and regenerating menadione (M) to repeat the cycle. Changes in the ratio of ferro- to ferricyanide are measured by a gold electrode (Figure 1). A similar cycle has been previously described in a cell free system.¹⁴ (C) Potentiometric measurements of menadione-mediated ferricyanide reduction by cells. Plotted are changes in the potential of the ferricyanide (10 μM starting concentration)/ferrocyanide (90 μM starting concentration) solution versus time. The dashed line shows data from a chamber containing no cells, while the solid line shows data from a chamber containing 4 × 10⁵ A20 B lymphoma cells. Menadione (10 μM) was added at *t* = 0. The sensing chamber was perfused with fresh media during the periods shown in white. The shaded boxes represent the no-perfusion (pump off) periods. The reduction rate is the rate of change in the measured potential during the last 10 s of the no-perfusion periods.

The rate-limiting step in this process (see Figure 2B) could *a priori* be intracellular menadione reduction, transport of menadione or menadiol across the plasma membrane, extracellular transfer of electrons from menadiol to ferricyanide, or an unexpected reaction (i.e., one not depicted in Figure 2B). To investigate these possibilities, the dependence of the reduction rate on ferri(o)cyanide concentration, cell number, and menadione concentration was measured (Figure 3). Although the measured reduction rate (μV s⁻¹) does depend on the ferri- and

ferrocyanide concentrations as dictated by the Nernst equation, for concentrations of ferri- and ferrocyanide >30 μM, the molar amount of ferricyanide reduction (μM s⁻¹) does not depend on the concentrations of either ferri- or ferrocyanide (Figure 3, parts A and B). This demonstrates that extracellular transfer of electrons from menadiol to ferricyanide is not rate limiting. Consistent with these results, the reduction rate increases linearly with increasing cell number, demonstrating that the rate-limiting step is cell dependent (Figure 3C). The rate of this step depends on menadione concentration according to Michaelis–Menten kinetics with *K_M* for menadione of approximately 2 μM in CHO cells (Figure 3D) and approximately 7 μM in L929 cells (data not shown), suggesting that it involves binding of menadione to a saturable catalyst. One candidate is the enzyme DT-diaphorase, which catalyzes transfer of electrons from either NADH or NADPH to quinones such as menadione with a *K_M* for menadione of approximately 2–8 μM.²²

To determine whether DT-diaphorase activity contributes to menadione reduction, four different cell lines were treated with the DT-diaphorase inhibitor dicumarol. Low concentrations of dicumarol (≤3 μM) have no effect on cellular metabolism as measured by acid release (Table 1). However, dicumarol causes a rapid decrease in the reduction rate of each cell line (Table 1, Figure 4A), consistent with inhibition of DT-diaphorase-catalyzed transfer of electrons from NAD(P)H to menadione.²³ While these results demonstrate that DT-diaphorase is involved in menadione reduction, they do not address the extent to which DT-diaphorase activity limits the rate of menadione reduction. To answer this question, the reduction rate of cells genetically engineered to express different levels of DT-diaphorase²⁴ was determined. Expression of DT-diaphorase enhances the menadione reduction rate of whole cells in our assay system roughly in proportion to the activity measured from cell lysates²⁴ (Figure 4B).

Further evidence for the menadione reaction cycle depicted in Figure 2B is the effect of addition of menadione on the rate of proton excretion by cells bathed in media containing ferri(o)cyanide. As depicted in Figure 2, when menadiol reacts with two molecules of ferricyanide, the products are menadione, two molecules of ferrocyanide, and two protons. Consistent with this reaction, addition of menadione to cells bathed in media containing ferri(o)cyanide enhances the rate of proton release (as measured by acid microphysiometry). In three different cell lines (L929, CHO, and CH27), the increase in the rate of proton release (μM s⁻¹) is approximately equal to the menadione-mediated rate of ferricyanide reduction (μM s⁻¹) (data not shown).

Glycolysis and the Pentose Phosphate Pathway. Menadione reduction requires a continuous supply of glucose (Figure 5A, Table 1). Glucose oxidation generates two main reduced species, NADH and NADPH (Figure 5B), both of which can donate electrons to quinones via DT-diaphorase. To determine which one is the major contributor to menadione reduction, we treated cells with inhibitors of the glycolytic versus the pentose phosphate pathway. In several different cell lines, inhibition of glycolysis with either fluoride²⁵ or iodoacetate²⁶ decreases the acid release rate (Table 1) but not the reduction rate (Figure

(22) Hall, J. M.; Lind, C.; Golvano, M. P.; Rase, B.; Ernster, L. *Structure and function of oxidation reduction enzymes: DT Diaphorase—Reaction mechanism and metabolic function*; Pergamon: Oxford, 1970; pp 433–444.

(23) Goodwin, C. J.; Holt, S. J.; Riley, P. A.; Downes, S.; Marshall, N. *J. Biochem. Biophys. Res. Commun.* **1996**, *226*, 935–941.

(24) Gustafson, D. L.; Beall, H. D.; Bolton, E. M.; Ross, D.; Waldren, C. A. *Mol. Pharmacol.* **1996**, *50*, 728–735.

(25) Pelster, B. *Am. J. Physiol.* **1995**, *269*, R793–R799.

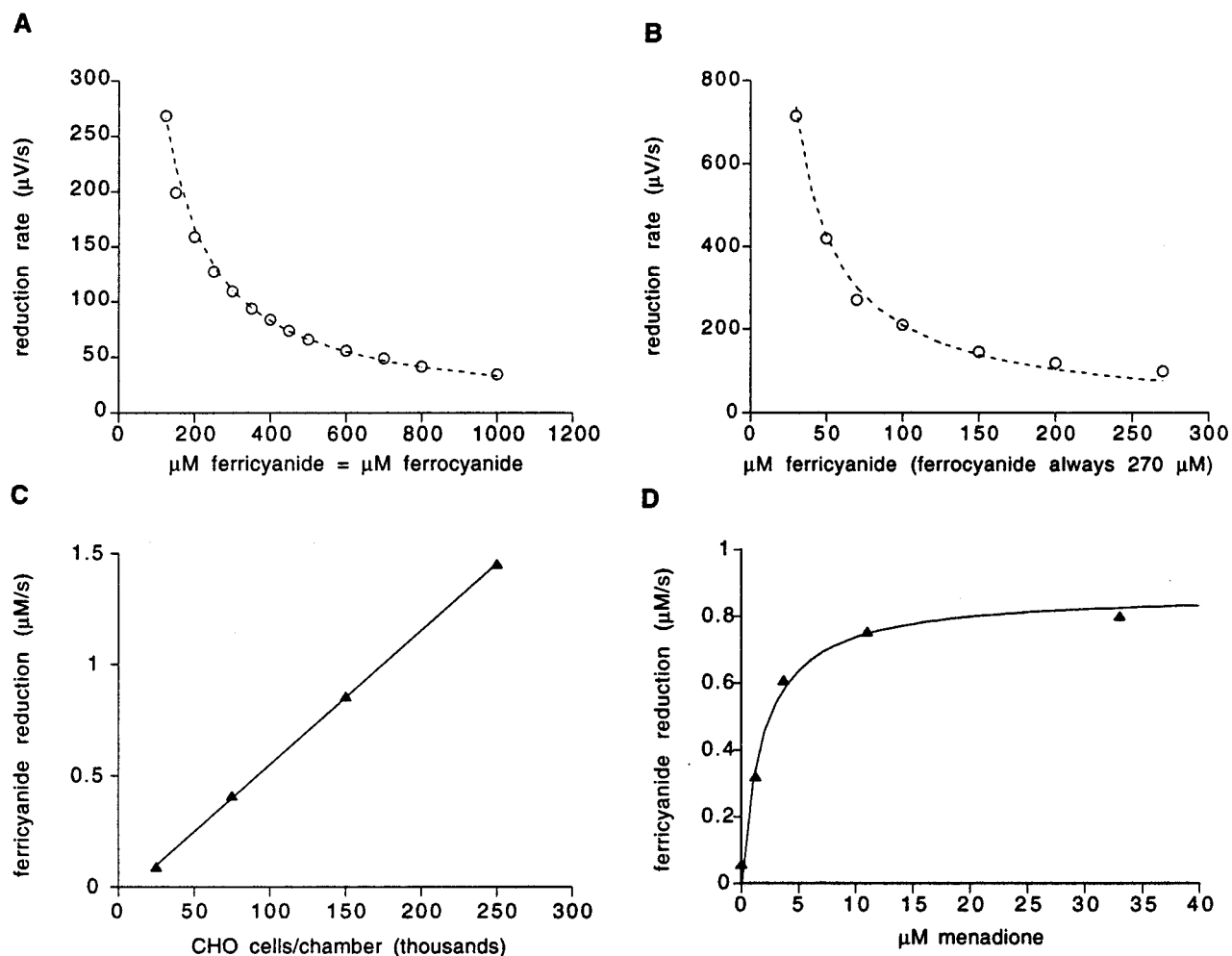


Figure 3. The measured ferricyanide reduction rate is proportional to the rate of cellular menadione reduction. (A and B) Effect of ferri(o)cyanide concentration on the measured reduction rate. Circles indicate experimental data points (measured in $\mu\text{V s}^{-1}$) as described in the experimental section. Dashed lines indicate theoretical values computed assuming a constant rate of conversion of ferricyanide into ferrocyanide independent of the ferri(o)cyanide concentration as described in the experimental section. In part A, the sensing chamber contained 2×10^5 CHO cells and calculations (dashed line) were based on a molar reduction rate of $0.65 \mu\text{M ferricyanide s}^{-1}$. In part B, the sensing chamber contained 10^5 CHO cells and calculations were based on a molar reduction rate of $0.4 \mu\text{M ferricyanide s}^{-1}$. (C) Effect of cell number on the reduction rate. Cells were perfused with media containing $10 \mu\text{M}$ menadione and $200 \mu\text{M}$ each of ferri(o)cyanide. The solid line indicates a linear regression fit to the experimental data, with a slope of $0.6 \mu\text{M ferricyanide s}^{-1}$ per 10^5 CHO cells. (D) Effect of menadione concentration on the reduction rate. The sensing chamber was loaded with 2×10^5 CHO cells and the initial solution contained $150 \mu\text{M}$ each of ferri(o)cyanide. The solid line indicates a Michaelis–Menten fit to the experimental data, with $V_{\text{max}} = 0.9 \mu\text{M ferricyanide s}^{-1}$ and $K_m = 1.8 \mu\text{M menadione}$. All experiments have been repeated at least three times and similar results have also been obtained by using either L929 fibroblasts or A20 B lymphoma cells.

Table 1. Changes in the Rates of Cellular Reduction and Acid Release in Response to Stimuli That Alter Cellular Metabolism^a

stimulus	CH27 redox	CHO redox	5C.C7 redox	L929 redox	CH27 acid	CHO acid	5C.C7 acid	L929 acid
dicumarol, 3 μM	-30	-60	-60	-80	0	0	0	0
no glucose	-60	-80	-80	-70	-70	-70	-20	-40
epiandrosterone, 200 μM	-40	-80	-90	-80	-20	-80	+/-	+/-
iodoacetate, 400 μM	0	0	0	0	-60	-60	-20	-60
fluoride, 5 mM	0	0	0	0	-60	-50	0	-30
oxamate, 5 mM	0	+90	0	0	-30	-50	0	-40
oxamate (postantimycin)	+30	+150	+10	0	-80	-80	-60	-80
rotenone, 10 μM	-20	-20	0	-10	+30	+10	+120	+70
antimycin A, 10 μM	+100	+70	+60	0	+20	+10	+100	+70
azide, 5 mM	+80	+70	+40	0	+20	+10	+120	+70

^a Reported data give the average percentage change in the reduction (redox) and acid release rate after 3 to 12 min of exposure of cells to the condition shown. The symbol +/- indicates that the initial response is a rate increase of >20%, followed by a decrease of >20%. Responses of less than 10% are reported as zero.

5C, Table 1). In contrast, inhibition of the pentose phosphate pathway with epiandrosterone²⁷ decreases the reduction rate (Figure 5C, Table 1) at least as much as it decreases the acid

release rate (Table 1). Thus, most menadione reduction is driven by NADPH produced by the pentose phosphate pathway. This is consistent with prior work demonstrating that the cellular

(26) Voet, D.; Voet, J. G. *Biochemistry*; John Wiley and Sons, Inc.: New York, 1995; pp 444–445.

(27) Grossman, S.; Budinsky, R.; Jollow, D. J. *Pharmacol. Exp. Ther.* 1995, 273, 870–877.

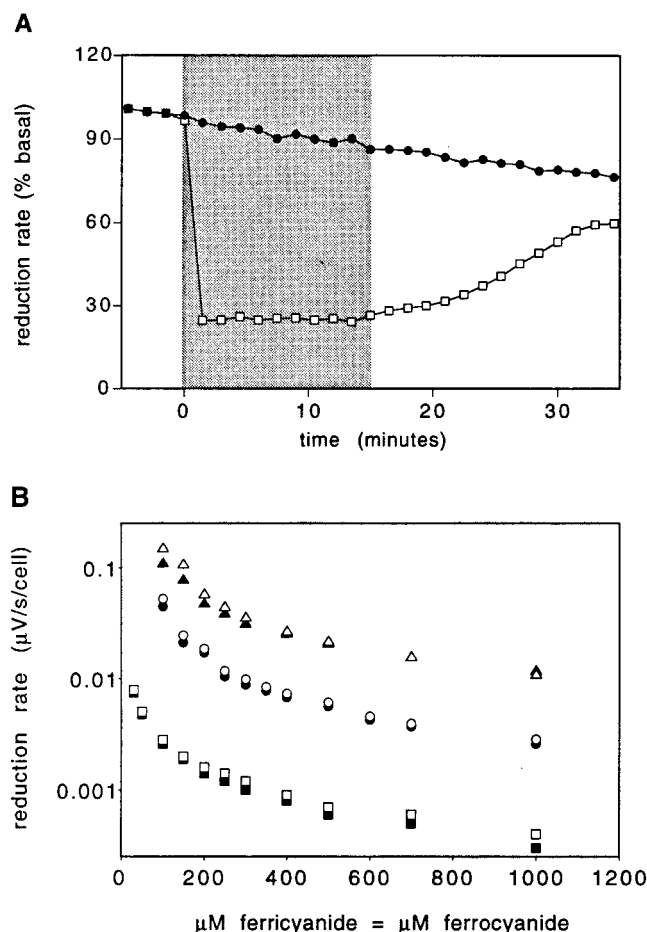


Figure 4. Correlation between DT-diaphorase activity and the menadione reduction rate. (A) Pharmacological inhibition of DT-diaphorase with 3 μM dicumarol (open squares). Dicumarol was added at time $t = 0$ for the duration indicated by the shaded box. Similar kinetics have been observed in three independent experiments with CHO cells, as well as with other cell lines (Table 1). (B) Effect of genetic over-expression of DT-diaphorase on the menadione reduction rate. The reduction rate of DT-diaphorase-transfected CHO cells with high and moderate levels of DT-diaphorase expression (triangles and circles, respectively) was compared with their parental CHO cell line (squares). Cells were perfused with media containing 10 μM menadione and the indicated concentrations of ferri(o)cyanide. Measurements were performed in duplicate.

NADH/NAD⁺ ratio is low, while the NADPH/NADP⁺ ratio is high.^{9–12}

In cells undergoing anaerobic metabolism, a low NADH/NAD⁺ ratio is maintained by lactate dehydrogenase, which regenerates NAD⁺ from NADH by reducing pyruvate to lactate (Figure 5B). In cell lines with a low rate of aerobic metabolism, blocking lactate dehydrogenase reduces the rate of glycolysis by depleting NAD⁺. This is evident as a decrease in the rate of acid release upon addition of oxamate, an inhibitor of lactate dehydrogenase activity²⁸ (Table 1). This effect of oxamate is enhanced by rendering cells almost completely anaerobic by inhibition of mitochondrial electron transport with antimycin A (Table 1). In contrast to decreasing the acid release rate, oxamate increases the reduction rate of anaerobic cells by blocking the transfer of electrons from NADH to pyruvate to form lactate, which does not react with menadione and is lost outside the cell (Figure 5D, Table 1). The increase in the reduction rate triggered by oxamate is due to accumulation of

NADH produced by glycolysis, as it is blocked by the glycolytic inhibitor iodoacetate (Figure 5D). Thus, the reduction rate is sensitive to the cellular content of both NADH and NADPH, with NADPH being the predominant electron donor under basal metabolic conditions. These characteristics make this method suitable for screening for novel inhibitors of cytoplasmic redox reactions, in particular those producing or consuming NADPH.²⁹

Mitochondrial Electron Transport. Structural analogues of ubiquinone, including menadione, can act as efficient electron donors and acceptors of the respiratory chain.^{30,31} We have used a series of well-known inhibitors of mitochondrial respiration³² to study the sensitivity of menadione reduction and oxidation to the activities of electron transport chain enzymes. Figure 6A shows the electron flow through the respiratory chain as well as the sites of inhibition by rotenone, antimycin A, and azide.

All three inhibitors increase the rate of cellular acid release (Table 1). This effect is consistent with cells switching from aerobic to anaerobic metabolism to fulfill their ATP demand.^{8,33} In contrast, depending on which step of the electron transport chain is blocked by the inhibitors, we observe opposing effects on the menadione reduction rate (Figure 6B). Rotenone, a specific inhibitor of complex I, blocks the transfer of electrons from NADH-Q-reductase to ubiquinone, leading to an accumulation of ubiquinone in its oxidized form. Consistent with inhibition of electron transfer from NADH to menadione, rotenone decreases the reduction rate (Figure 6B, Table 1). Antimycin A inhibits the transfer of electrons from ubisemiquinone radicals to cytochrome b_H in complex III of the electron transport chain. Upon addition of antimycin, menadiol can no longer donate its electrons to cytochrome b , leading to an increase in the rate of transfer of electrons to extracellular ferricyanide (Figure 6B, Table 1). A similar effect to that of antimycin is observed with azide, which blocks electron transfer from heme a_3 in complex IV to O₂. Electrons can no longer be transferred to O₂ leading to a backup of the electron transport chain. As a consequence, menadiol accumulates and its electrons are transferred to extracellular ferricyanide (Figure 6B, Table 1). Consistent with antimycin and azide both blocking the same pathway, cells pretreated with antimycin show little change in their reduction rate upon addition of azide (data not shown).

To investigate further the effect of mitochondrial O₂ reactions on menadione reduction and oxidation, we measured the cellular reduction rate under low oxygen conditions. These experiments also confirm that the thermodynamically favorable transfer of electrons from menadiol to O₂ is too slow in the absence of enzymatic catalysis to affect the measurements.^{19,21,34,35} Depletion of oxygen to 5% of atmospheric concentration by argon bubbling has no effect on cellular acid release or reduction rates (data not shown). Nearly complete oxygen removal by an enzymatic method (see Experimental Section) recapitulates the effects of antimycin A and azide on the CHO reduction rate

(29) A small (approximately 20 compound) screen in our laboratory has identified a novel effect of the potassium channel blocker clofilium as a potent inhibitor of redox metabolism; Rabinowitz, J. D.; Rigler, P.; Carswell-Crumpton, C.; Beeson, C.; McConnell, H. M. *Life Sci.* **1997**, *61*, PL87-PL94 and unpublished results.

(30) Kröger, A.; Klingenberg, M. *Eur. J. Biochem.* **1973**, *39*, 313–323.

(31) Ragan, C. I. *Biochim. Biophys. Acta* **1976**, *456*, 249–290.

(32) Stryer, L. *Biochemistry*; W. H. Freeman and Company: New York, 1995; pp 533–544.

(33) Miller, D. L.; Olson, J. C.; Parce, J. W.; Owicki, J. C. *Biophys. J.* **1993**, *64*, 813–823.

(34) Ohnishi, T.; Yamazaki, H.; Iyanagi, T.; Nakamura, T.; Yamazaki, I. *Biochim. Biophys. Acta* **1969**, *172*, 357–369.

(35) Nakamura, M.; Hayashi, T. *J. Biochem.* **1994**, *115*, 1141–1147.

(28) Zollner, H. *Handbook of Enzyme Inhibitors*; VCH Verlagsgesellschaft: Weinheim 1993; pp 301 and 888.

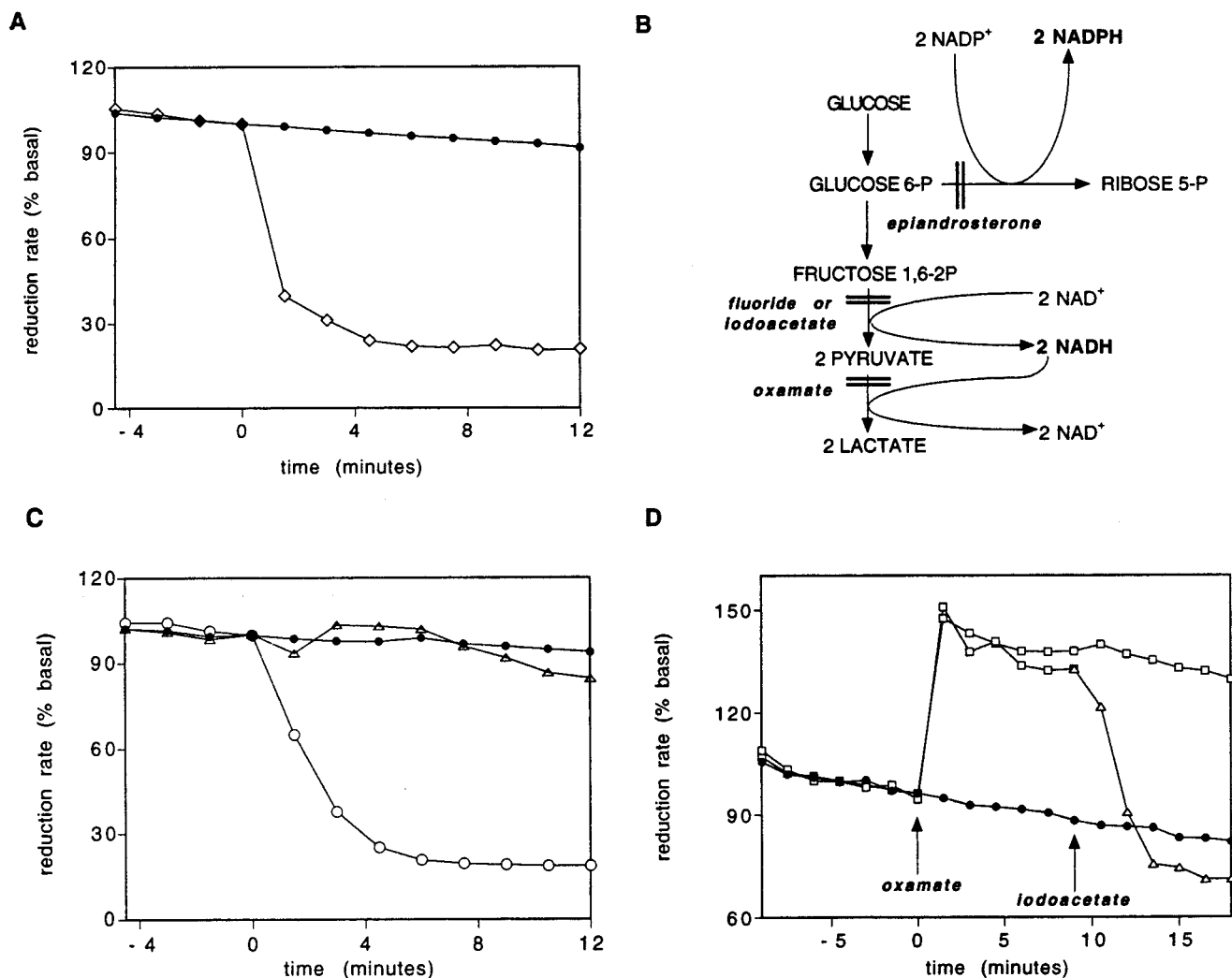


Figure 5. Contribution of cytosolic glucose metabolism to menadione reduction. (A) Removal of glucose. CHO cells were deprived of glucose starting at $t = 0$ (open diamonds, glucose deprivation; closed circles, control). Similar kinetics have been observed in three independent experiments with CHO cells, as well as with other cell lines (Table 1). (B) Schematic depicting reactions of the glycolytic pathway (vertical) and the pentose phosphate pathway (horizontal) resulting in pyridine nucleotide oxidation or reduction. Reduced nucleotides are in bold. Pharmacological inhibitors of the pathways are in italics. (C) Pharmacological inhibition of the pentose phosphate pathway with $200 \mu\text{M}$ epiandrosterone (open circles) or of glycolysis with 1 mM iodoacetate (triangles). Drugs were added at time $t = 0$ for the duration of the experiment. Similar kinetics have been observed in three independent experiments with CHO cells, as well as with other cell lines (Table 1). (D) Inhibition of lactate dehydrogenase in CHO cells with 5 mM oxamate (open symbols), followed by inhibition of glycolysis with 1 mM iodoacetate (squares, no iodoacetate; triangles, iodoacetate). Drugs were added at the times indicated by the arrows and continued for the duration of the experiment.

(Figure 6C). To confirm that this result is due to oxygen removal rather than the enzymes added or their byproducts, media was passed through the gas-permeable membrane of the microphysiometer debubbler.⁸ Under these conditions, O_2 redissolves in the media and we observe no change in the reduction rate (Figure 6C). Thus by using oxygen-depleted media and specific inhibitors of complexes I, III, and IV, we are able to correlate the cellular reduction rate with the activity of each of these enzyme complexes.

Signal Transduction Cascades. In chloroplasts, reducing power generated by the light reactions of photosynthesis reduces several targets including thioredoxin, a 12 kD protein with two exposed cysteine residues separated by a conserved glycine-proline spacer. Thioredoxin subsequently reduces targets including chloroplast mRNA binding proteins and the enzymes catalyzing the dark reactions of photosynthesis.^{2,4} In this way chloroplast protein expression and activity is tuned to the amount of light available. While the activities of analogous proteins in the cytoplasm and nuclei of eukaryotic cells can also be

regulated by redox reactions,^{3,5,6} the way in which the redox states of these proteins are determined remains largely unknown.

Menadione reduction is sensitive to the activities of several cellular enzymes which might potentially be regulated by signal transduction cascades. These include glucose 6-phosphate dehydrogenase, lactate dehydrogenase, DT-diaphorase, and enzymes of the mitochondrial electron transport chain. Because the methodology described above can detect changes in the rate of menadione reduction of as little as 3%, it is suitable for investigation of the effects of hormonal stimuli on cellular redox activity.

The effects of several different signal transduction cascades on the rate of cellular acid release and menadione reduction are summarized in Table 2. Examples of kinetics of the reduction rate responses are shown in Figure 7. All of the tested stimuli increase the acid release rate of their target cell. This is likely because each pathway triggers glycolysis, either directly (e.g., insulin) or by enhancing the rate of cellular ATP consumption. In contrast, three stimuli increase the reduction

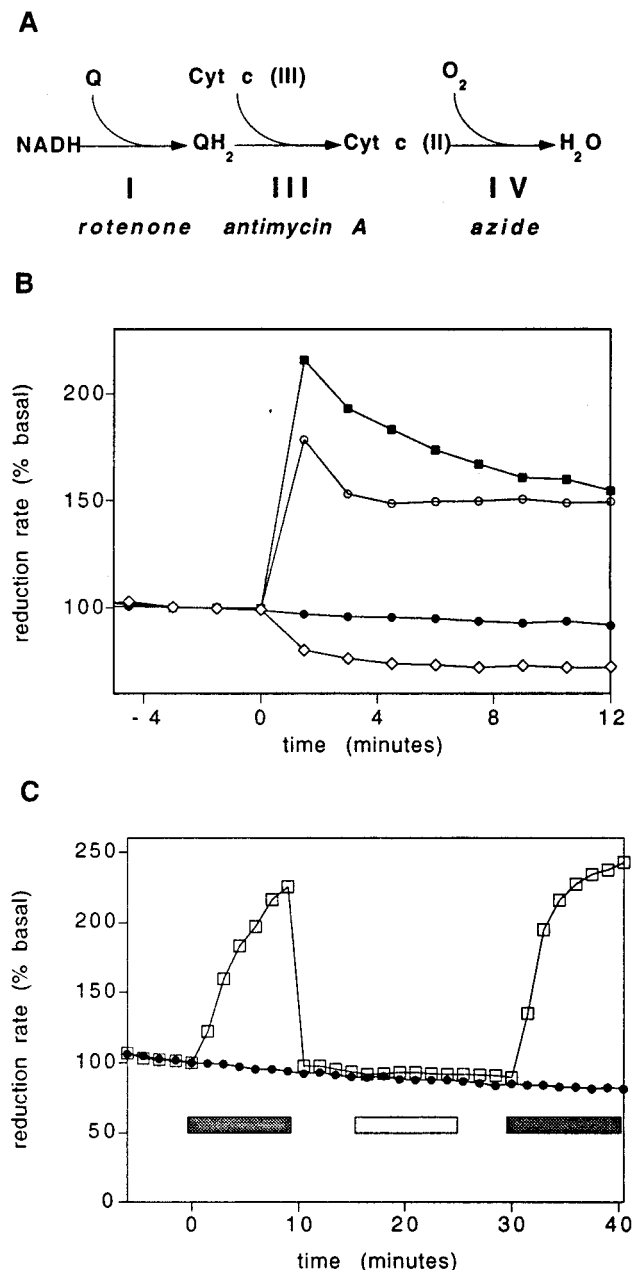


Figure 6. Effect of reactions of the mitochondrial electron transport chain on the menadione reduction rate. (A) Schematic depicting reactions of the mitochondrial electron transport chain which carry electrons from NADH to oxygen. Under physiological conditions Q is ubiquinone, but menadione can undergo the same reactions.^{30,31} Pharmacological inhibitors of each complex are in italics. (B) Pharmacological inhibition of complex I with 10 μ M rotenone (open diamonds), complex III with 2 μ M antimycin A (open circles), and complex IV with 5 mM azide (closed squares). Drugs were added at time $t = 0$ for the duration of the experiment. Similar kinetics have been observed in three independent experiments with CHO cells, as well as with other cell lines (Table 1). (C) Effect of enzymatic removal of oxygen. CHO cells received oxygen-depleted media (see Experimental Section) as indicated by the shaded horizontal bars. The open horizontal bar indicates exposure to media, which was first deoxygenated and subsequently reoxygenated by passing through the microphysiometer debubbler.

rate and three other stimuli decrease this rate. Each response follows a consistent kinetic pattern over a broad range of menadione (Figure 7A) and ferri(o)cyanide concentrations (data not shown). These data demonstrate that the tested hormonal

stimuli trigger specific, regulated changes in cellular redox metabolism.

Triggering of each of the tested receptors which couples to the phospholipase C signaling pathway (ATP purinergic receptor, M1 muscarinic receptor, and T cell receptor) results in increases in the menadione reduction rate. In contrast, the other test stimuli all decrease the menadione reduction rate. These data suggest that a common feature of the phospholipase C signaling pathway, which causes increases in intracellular calcium and protein kinase C activation, is either enhancement of enzymatic pathways leading to menadione reduction or inhibition of pathways resulting in menadiol oxidation.

Comparison to Other Methods for Measuring Cellular Redox. As stated in the Introduction, biochemical techniques exist for direct quantitation of most important cellular redox couples such as NAD^+/NADH , $\text{NADP}^+/\text{NADPH}$, cystine/cysteine, and GSSG/GSH. Measurements of pyridine nucleotides are based on the characteristic absorption and fluorescence of NAD(P)H. Specific measurements of NAD^+ can be obtained by measuring the absorption of cell lysates before and after conversion of NAD^+ to NADH by alcohol dehydrogenase with ethanol as the reducing agent.^{9,10} Similar methods allow determination of NADH, NADP^+ , and NADPH. Measurements of cystine, cysteine, GSSG, and GSH are based on the reactivity of the thiol moiety and the ability to separate these species by using reverse-phase high performance liquid chromatography (rpHPLC)³⁶ or cellulose high performance thin-layer chromatography (HPTLC).¹³ Less specific detection of cellular thiols can be obtained in live cells by using membrane-permeable compounds such as bimanes which are fluorescent upon thiol conjugation.³⁷ Cellular redox activity can be detected by using the dye Alamar blue,³⁸ although this approach has not yet been used to make kinetic measurements of intracellular redox activity similar to those in this report. Detection of some cellular reactions involving free radicals can be achieved by using membrane-permeable fluorescent compounds which either increase in fluorescence or are retained in cells after reacting with radicals such as superoxide.³⁹ Paramagnetic resonance spectroscopy has been used to study free radical reactions of nitric oxide in cells.⁴⁰

An important difference between the potentiometric method presented in this report and the standard biochemical assays for NAD(P)H is that our method measures the rate of cellular reactions, rather than the steady-state concentration of a particular biochemical species. In this way, the standard spectroscopic methods for measuring pyridine nucleotides in cell extracts and the potentiometric method described here for live cells are complementary rather than redundant. Similarly, our measurement of the rates of cytoplasmic and mitochondrial redox reactions should provide a useful complement to measurements of cellular thiol and free radical reactions.

The present work makes no claim that the method described is the simplest, most convenient, or most sensitive one for measuring the rates of cellular redox reactions. One might imagine that dyes or other electrochemical methods could provide similar information. Nevertheless, this report, by

(36) Carelli, S.; Ceriotti, A.; Cabibbo, A.; Fassina, G.; Ruvo, M.; Sitia, R. *Science* **1997**, *277*, 1681–1684.

(37) Bellomo, G.; Palladini, G.; Vairetti, M. *Microsc. Res. Technol.* **1997**, *36*, 243–252.

(38) Ahmed, S. A.; Gogal, R. M.; Walsh, J. E. *J. Immunol. Methods* **1994**, *170*, 211–224.

(39) Goossens, V.; Grooten, J.; De Vos, K.; Fiers, W. *Proc. Natl. Acad. Sci. U.S.A.* **1995**, *92*, 8115–8119.

(40) Vanin, A. F.; Malenkova, I. V.; Serezhenkov, V. A. *Nitric Oxide: Biol. Chem.* **1997**, *1*, 191–203.

Table 2. Effect of Signal Transduction Cascades on Rates of Cellular Reduction and Acid Release^a

cell type	transfected receptor	stimulus	control	redox	acid
CHO	none	ATP, 10 μ M	none	+10	+30
CHO	none	insulin, 400 nM	glucagon, 400 nM	-6	+50
CHO	none	<i>cis</i> -9,10-octadecenoamide, 50 μ M	<i>trans</i> -9,10-octadecenoamide, 50 μ M	-10	+16
CHO	type I muscarinic acetyl choline	carbachol, 10 μ M	carbachol (10 μ M) + atropine (10 μ M)	+30	+40
CHO	nociceptin	nociceptin, 100 nM	cells pretreated with pertussis toxin	-8	+40
5C.C7 T cell	none	anti-CD3, 2 μ g/mL	control IgG	+12	+100

^a Cells were treated with the indicated stimuli for 9 min, and the maximum percentage change in the acid release and reduction rate during this time period was recorded. The control stimuli never resulted in any detectable ($\geq 3\%$) change in either the acid release or the reduction rate. Each experiment was performed at least three times, with the direction (increase vs decrease) and kinetics of the response consistent each time. The magnitudes of the responses were consistent on any given day (standard deviations $< 20\%$ of the observed response), but sometimes (especially in the case of M1 signaling) varied considerably between days.

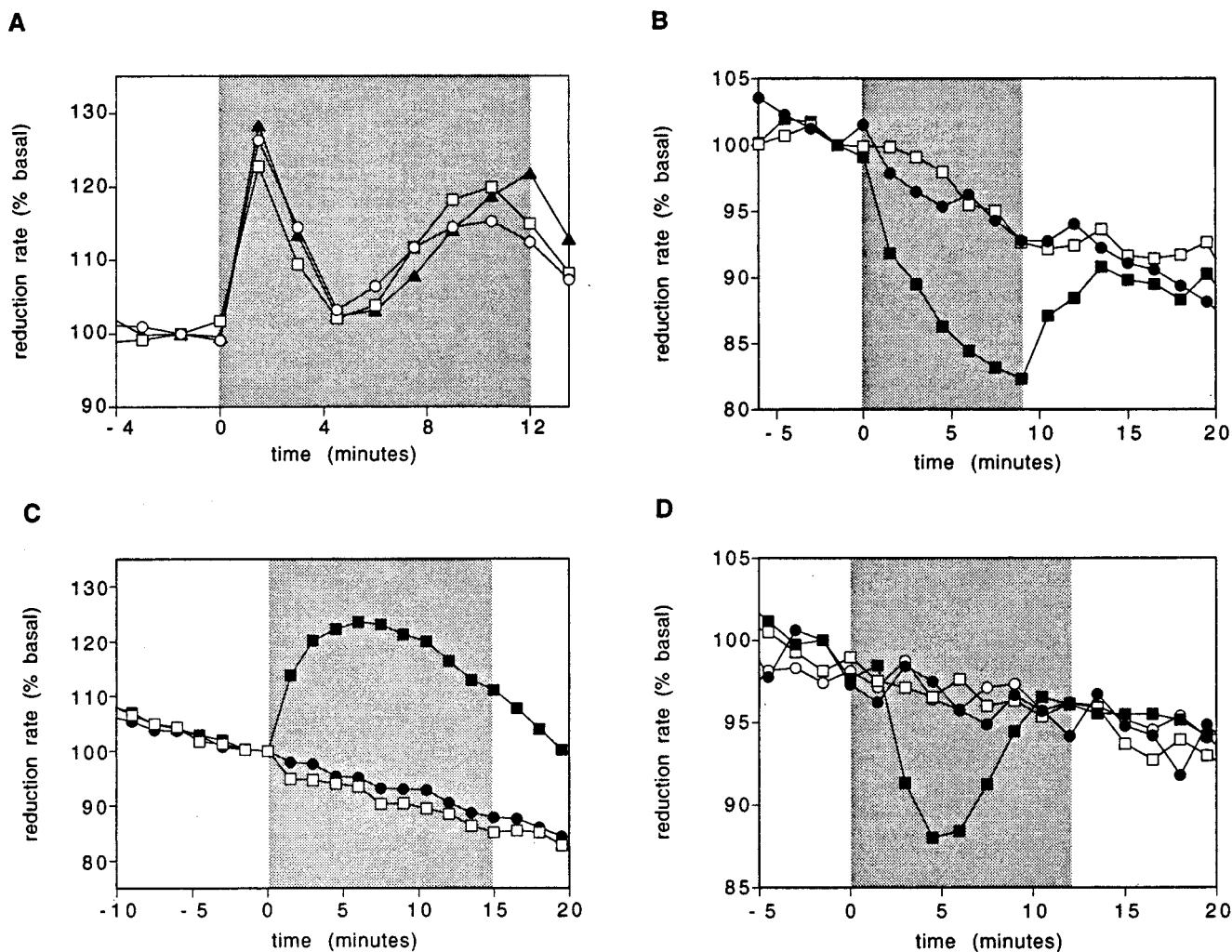


Figure 7. Different signal transduction cascades have opposing effects on the CHO cell reduction rate. (A) Response of CHO cells to 10 μ M ATP when perfused with media containing either 33 μ M (triangles), 10 μ M (squares), or 3.3 μ M (circles) menadione. (B) Response of CHO cells to the sleep lipid⁴⁴ *cis*-9,10-octadecenoamide (50 μ M, closed squares) or its less active isomer *trans*-9,10-octadecenoamide (50 μ M, open squares). (C) Response of CHO cells transfected with the type I muscarinic acetyl choline receptor to the muscarinic agonist carbachol (10 μ M) in the presence (open squares) or absence (closed squares) of the muscarinic antagonist atropine (10 μ M). (D) Response of CHO cells transfected with the nociceptin receptor to 100 nM nociceptin peptide⁴³ (closed symbols, nociceptin peptide; open symbols, no peptide). The response of cells pretreated overnight with 100 ng/mL of pertussis toxin is shown with circles. Cells not receiving toxin are shown as squares. In parts A, B, C, and D, the duration of drug exposure is indicated by the shaded area.

describing one practical and sensitive method for kinetic measurements of intracellular redox activity, provides a starting point for such efforts.

Conclusions

In this report, we demonstrate that the carrier mediator menadione can effectively couple the interior of cells to an extracellular redox couple. In the cytoplasm, the glycolytic and

pentose phosphate pathways produce NADH and NADPH, which reduce menadione to menadiol in reactions catalyzed by DT-diaphorase. In mitochondria, enzymes of the electron transport chain react with menadione and menadiol. Addition of hormonal stimuli produces changes in redox metabolism which are reflected within minutes in the reduction rate. Because menadione can react with multiple cellular substrates, pinpointing the biochemical basis for these signals

is challenging. An important future task is identifying the biochemical reactions responsible for these signals. One possible approach to this problem is to study genetically engineered cells which either lack or overexpress key enzymes. Another is to develop other probes of cellular redox reactions, which are more specific than menadione, or respond to different cellular redox couples from menadione. A second future task concerns the application of this method for the screening of chemical libraries for compounds affecting redox metabolism.

Experimental Section

Cell Culture. Cells were grown in RPMI media 1640 supplemented with 10% fetal calf serum (HyClone, Logan, UT), 10 mM HEPES (4-(2-hydroxyethyl)-1-piperazineethanesulfonic acid), 1 mM sodium pyruvate, 20 μ M 2-mercaptoethanol (2-hydroxy-1-ethanethiol), and non-essential amino acids (Irvine Scientific, Santa Ana, CA), pH 7.4 at 37 °C and 5% carbon dioxide. L929 cells and Chinese Hamster Ovary (CHO) cells were obtained from American Type Tissue Culture. M1 muscarinic receptor-transfected CHO cells and DT-diaphorase-transfected CHO cells were the generous gifts of Jack Owicki and Daniel Gustafson, respectively, and have been previously described.^{7,24} CHO cells transfected with the nociceptin receptor were the generous gift of Gary Wada and are currently commercially available from Molecular Devices (Sunnyvale, CA). 5C.C7 T lymphocytes were derived from the 5C.C7 T cell receptor transgenic mouse⁴¹ and purified and maintained in vitro as previously described.⁴² A20 and CH27 cells are commonly used murine B lymphoma cell lines.

Compounds. Potassium ferrocyanide and potassium ferricyanide (ACS quality reagents), menadione, sodium fluoride, sodium oxamate, rotenone, sodium azide, sodium cyanide, glucose oxidase (EC 1.1.3.4 type VII from *Aspergillus niger*), catalase (EC 1.11.1.6 from bovine liver), atropine, carbachol, ATP, insulin, and pertussis toxin were purchased from Sigma. Dicumaryl, iodoacetate, and epiandrosterone were purchased from Aldrich. Antimycin A was purchased from ICN. Nociceptin peptide⁴³ was purchased from Research Biochemicals International. 9,10-Octadecenoamide compounds⁴⁴ were the kind gift of Richard Lerner and Benjamin Cravatt. Anti-mouse CD3 monoclonal antibody 145-2C11⁴⁵ was grown from hamster 145-2C11 hybridomas in our laboratory and purified by protein A-Sepharose affinity chromatography.

Acid Microphysiometry. Cellular acid release was measured as previously described.⁸ Cells (0.3×10^6 to 15×10^6 , depending on experimental conditions and cell type) are collected by centrifugation and the cell pellet resuspended in a small volume (typically 80 μ L) of RPMI 1640 medium which is mixed with one-fourth the volume (typically 20 μ L) of low temperature melting agarose (Molecular Devices, Sunnyvale, CA). The 20% agarose mixture (7 μ L) is immediately spotted onto the membrane of a Cytosensor cell capsule. After 5 min at 4 °C to allow the agarose to solidify, the cell capsule is assembled and loaded in a microphysiometer sensing chamber containing a pH-sensitive silicon-based electrode. The chamber is maintained at 37 °C and perfused (1 μ L s⁻¹) with RPMI 1640 containing 1 mg/mL endotoxin-free bovine serum albumin (Calbiochem, San Diego, CA) and no bicarbonate or serum, pH 7.4. The instrument is calibrated to zero volts while the chamber is being perfused. Following calibration, measurements are made by perfusing the chamber for 58-s intervals, followed by 32-s intervals without perfusion. The rate of

change in the potential measured by the pH-sensing electrode during seconds 10–30 of the no-perfusion period defines the acid release rate. Optimal basal acid release rates are 60–200 μ V s⁻¹. Achieving basal rates in this range requires an appropriate match between the buffering capacity of the media and the cell number and type. Special RPMI media containing 1 mM phosphate (Molecular Devices, Sunnyvale, CA) was used for 5C.C7 T cells (0.3×10^6 to 1×10^6 /chamber) and for experiments using low numbers (0.3×10^5 to 1×10^5 /chamber) of CHO, L929, or CH27 cells. The large number of 5C.C7 cells is required because they are much less metabolically active than the transformed cell lines. Experiments with higher numbers (3×10^5 to 6×10^5 /chamber) of CHO, L929, or CH27 cells were performed with use of standard RPMI 1640 media containing 10 mM phosphate.

Redox Microphysiometry. The procedure for measuring the cellular reduction rate parallels the measurement of the acid release rate and measurements of both types were frequently performed in parallel. In these cases, reduction rate experiments were performed as rapidly as possible following capsule loading to mitigate alterations in cell physiology due to exposure to menadione, with acid release experiments often following the reduction rate experiments. Preparation of the cell capsule is identical in both cases. Once the cell capsule is assembled as described above, it is loaded in a microphysiometer sensing chamber with a gold electrode.¹⁵ Prior to each experiment the chamber and electrode are washed with distilled water and equilibrated with redox medium consisting of phosphate buffered saline (145 mM Na⁺, 4 mM K⁺, 1 mM Mg²⁺, 1 mM Ca²⁺, 143 mM Cl⁻, 10 mM phosphate, pH 7.4) supplemented with 10 mM glucose, 20 mM HEPES, 1 mg/mL of endotoxin-free bovine serum albumin, and micromolar concentrations of ferricyanide and ferrocyanide (30–300 μ M of each unless otherwise indicated). In this medium ferri(o)cyanide is the only redox agent, glucose is the only carbon source, and pH is buffered by both the phosphate and HEPES. Once loaded, the chamber is maintained at 37 °C and perfused 1 μ L s⁻¹ with redox medium. The instrument is calibrated to zero volts while the chamber is being perfused in the absence of menadione. Following calibration, measurements are made by switching into redox media containing micromolar menadione (10 μ M unless otherwise indicated). Following addition of menadione, measurements were performed as rapidly as possible (within 12 minutes for signal transduction experiments, and within 1 hour for addition of metabolic inhibitors). As in the case of acid release measurements, the chamber is perfused for 58-s intervals, followed by 32-s intervals without perfusion. The rate of change in the potential measured by the gold electrode during seconds 20–30 of the no-perfusion period defines the reduction rate. The longer delay between turning off the pump (stopping perfusion) and the rate measurement in redox than in acid mode is because the gold electrode does not equilibrate with the extracellular ferri(o)cyanide redox pair as rapidly as the pH-sensing electrode equilibrates with protons. Optimal basal reduction rates are 400–1000 μ V s⁻¹. Achieving basal rates in this range requires an appropriate match between the ferri(o)cyanide concentration and the cell number and type. Detailed data on appropriate ferri(o)cyanide concentration choice for CHO and DT-diaphorase-transfected CHO cells is contained in Figures 3 and 4, respectively. For given ferri(o)cyanide concentrations, a reduction rate comparable to the CHO cell reduction rate can be achieved by using 10-fold higher numbers of 5C.C7 T cells, 3-fold higher numbers of CH27 cells, and 20-fold lower numbers of L929 cells.

Conversion between Molar, Potential, and Percentage Rates. In Figure 3, parts A and B, the dashed lines represent the computed relationship between changing the ferri(o)cyanide concentration and the reduction rate (measured in μ V s⁻¹), assuming that the rate of ferricyanide reduction (μ M s⁻¹) is independent of the amount of ferri(o)cyanide added. Computations are based on the Nernst equation:

$$y = (59 \times 10^3) \log\left[\frac{(b+x)/(a-x)}{(b/a)}\right]$$

where y is the measured reduction rate (μ V s⁻¹), x is the molar reduction rate (μ M s⁻¹), a is the initial ferricyanide concentration (μ M), and b is the initial ferrocyanide concentration (μ M). These computations are only an approximation because they do not include a correction for differences between concentrations and activities. In Figure 3, parts

(41) Seder, R. A.; Paul, W. E.; Davis, M. M.; Fazekas de St. Groth, B. *J. Exp. Med.* **1992**, *176*, 1091–1098.

(42) Beeson, C.; Rabinowitz, J.; Tate, K.; Gütgemann, I.; Chien, Y.; Jones, P. P.; Davis, M. M.; McConnell, H. M. *J. Exp. Med.* **1996**, *184*, 777–782.

(43) Meunier, J. C.; Mollereau, C.; Toll, L.; Suaudeau, C.; Moisand, C.; Alvinerie, P.; Butour, J. L.; Guillemot, J. C.; Ferrara, P.; Monsarrat, B.; Mazarguil, H.; Vassart, G.; Parmentier, M.; Costentin, J. *Nature* **1995**, *377*, 532–535.

(44) Cravatt, B. F.; Prospero-Garcia, O.; Siuzdak, G.; Gilula, N. B.; Henriksen, S. J.; Boger, D. L.; Lerner, R. A. *Science* **1995**, *268*, 1506–1509.

(45) Leo, O.; Foo, M.; Sachs, D. H.; Samelson, L. E.; Bluestone, J. A. *Proc. Natl. Acad. Sci. U.S.A.* **1987**, *84*, 1374–1378.

C and D, the reduction rate measured in $\mu\text{V s}^{-1}$ has been converted to $\mu\text{M ferricyanide s}^{-1}$ by using the Nernst equation above. In Figures 4–7 and Tables 1 and 2, data are reported as a percentage of the basal acid release or reduction rate, based on the formula $P(t) = 100V(t)B^{-1}$ where $P(t)$ is the percent reduction rate, $V(t)$ is the reduction rate in $\mu\text{V s}^{-1}$, and B is the average reduction rate in $\mu\text{V s}^{-1}$ during the 5 min prior to addition of the test compound. In all figures, closed circles represent cells never exposed to any drug.

Oxygen Removal. Oxygen was removed by argon bubbling followed by addition of glucose oxidase (2 U/mL) and catalase (2×10^4 U/mL). Glucose oxidase catalyzes the reaction of glucose and O_2 to form gluconate and H_2O_2 . The large excess of catalase eliminates the H_2O_2 formed in this reaction. In control experiments, addition of catalase alone did not affect the reduction rate while treatment with H_2O_2 , either directly or by addition of glucose oxidase in the absence of catalase, produced qualitatively different effects from O_2 depletion.

Menadione–Thiol Reactions. Compared to unsubstituted quinones, menadione (2-methyl-1,4-naphthalenedione) does not readily undergo most addition reactions.²⁰ However, the 2-methyl substituent does not markedly interfere with addition of sulfhydryl compounds.²⁰ Therefore, we were concerned with the rate at which menadione reacts with the sulfhydryl groups of proteins, peptides, and small molecules found inside cells, and the potential effect of these reactions on our measurements. As a prototypical sulfhydryl-containing cellular compound, we selected glutathione (γ -glutamylcysteinylglycine), as it is expressed at millimolar concentrations within cells. To investigate the reaction between GSH and menadione, the time course of the reaction

was monitored by rpHPLC. Over a time period of approximately 1 h, a solution of 200 μM menadione and 1 mM GSH reacted to yield a compound of intermediate hydrophobicity, presumably the conjugate. Based on these experiments, we compute a reaction rate of approximately $0.4 \text{ M}^{-1} \text{ s}^{-1}$ at 37 °C, pH 7.4, consistent with literature data on this type of reaction.²¹ These data suggest that while addition of micromolar concentrations of menadione can significantly alter cellular sulfhydryl groups over hours, 10 μM menadione does not significantly react with cellular thiols over the time course of our experiment. This assertion is supported by direct measurements of the effect of menadione on cellular GSH and protein thiols.^{17,46,47}

Acknowledgment. We thank colleagues at Molecular Devices Corporation, especially Dean Hafeman, Gary Wada, Jeff Libby, and Jack Owicki, for the gold electrodes and advice on microphysiometry. In addition, we thank Daniel Gustafson for the generous gift of the DT-diaphorase transfected cell lines and Richard Lerner and Benjamin Cravatt for the 9,10-octadecenoamide compounds. This work has been supported by the Medical Scientist Training Program (J.R.) and grants from the National Institutes of Health to H.M.M.

JA973560F

(46) McDuffee, A. T.; Senisterra, G.; Huntley, S.; Lepock, J. R.; Sekhar, K. R.; Meredith, M. J.; Borrelli, M. J.; Morrow, J. D.; Freeman, M. L. *J. Cell. Physiol.* **1997**, *171*, 143–151.

(47) Wefers, H.; Sies, H. *Arch. Biochem. Biophys.* **1983**, *224*, 568–578.